

SHELL COLLISION INDUCED KILO-HERTZ QUASI-PERIODIC OSCILLATION IN X-RAY BINARIES

BI-PING GONG¹, YA-PING LI²

¹School of Physics, Huazhong University of Science and Technology, Wuhan 430074, China and

²Department of Astronomy and Institute of Theoretical Physics and Astrophysics, Xiamen University, Xiamen, Fujian 361005, China

Draft version September 27, 2018

ABSTRACT

Twin kilo-Hertz Quasi-periodic oscillation with ratio 3/2 has been found in some compact sources, which is believed to be related with their innermost regions of accretion disks, and hence carrying information of gravity in strong regime. However, more complicated phenomena have been revealed, e.g., the twin kilo-Hertz Quasi-periodic oscillation of 4U 1820-20 start increasing at certain spectral state and then saturate upon reaching certain level. Moreover, such quasi-periodic oscillation is not uniform and has multiple peaks, which displays random feature. This letter suggests that these challenges could be easy to understand if the quasi-periodic oscillation originates in jets of compact objects. With a seed periodicity originating in either neutron star spin or accretion, shell collision develops in jet. The corresponding twin kilo-Hertz quasi-periodic oscillations automatically carry random feature, vary in frequency; and couple with luminosity, spectral properties, which well account for the observation of 4U 1820-30. New quasi-periodic oscillation of 4U 1820-30 is predicted, which can test the validity of this model. And the scenario is applicable to other compact object like AGN.

Subject headings: stars: neutron—X-rays: binaries—X-rays: individual (4U1820-30)

1. INTRODUCTION

Observations starting in 1996 with the Rossi X-ray Timing Explorer could detect faster variability, and it was found that neutron stars (NSs) and black holes (BHs) emit X-rays displaying quasi-periodic oscillation (QPO) with frequencies up to 1000 Hertz (Hz) or so, which is believed to be related with the accretion flow around NSs and BHs very close to the compact object and hence can test general relativistic theory in strong gravity regime. However, more complicated phenomena revealed in some X-ray binary systems led to no consensus on the origin of these high frequency QPOs, nor on what physical parameters determine these QPOs.

The source 4U 1820-30 is an atoll low mass X-ray binary (LMXB) in the globular cluster NGC 6624. Two simultaneous kHz QPOs were detected in the persistent flux from 4U1820-30 (Zhang et al. 1998). The source 4U 1820-30 undergoes a regular 176 day accretion cycle (Priedhorsky & Terrell 1984), which is further reported to be 172.780 days by Simon (2003).

The source switches between low- and high-luminosity states, which differ by a factor of 3 in their X-ray luminosity. In spectral color-color diagram (CCD), this corresponds to the evolution from the island, lower banana, to upper banana branches. As count rate increases from 1600 to 3200 count/s and above, the QPO frequency increases linearly with count rate below 2500 counts/s and then saturated while the flux of the source is still increasing (Zhang et al. 1998).

There is a gap in the distribution of QPO low frequencies between 600 and 650 Hz (Belloni et al. 2005; Barret & Boutelier 2008). Moreover, the distribution of twin kHz QPOs are not uniform and have multiple peaks, which display random feature (Belloni et al. 2005).

Various theoretical models have been proposed to account for kHz QPO signals (Miller et al. 1998; Lamb & Miller 2001; Abramowicz et al. 2003; Klis et al. 1997). Although each model has merit in some aspects. They

are still challenged by following facts: (a) evolution and saturation of QPO frequency (Zhang et al. 1998); (b) the random feature displaying as multiple peaks of QPOs (Belloni et al. 2005); (c) correlation of such an evolving QPO with CCD; and (d) with the circle of long-term activity of a source, like 176 days of 4U1820-30.

This letter directly confronts these challenges. With a seed periodicity at the central engine, shell collision occurs in jet, which can be treated by the technique applied in GRB.

Consequently, the power density spectrum (PDS) response of such a collision can be a twin kHz QPOs expected by observations. Furthermore, the evolution of such a twin QPOs automatically correlates with luminosity and spectral properties of the source. The model is described in Section 2 which is applied to 4U1820-30 in Section 3, and corresponding prediction is made in Section 4.

2. SHELL COLLISION IN JET

The jets of NS can behave much like jets from black holes. Typically, collimated matter is blasted into space like water from a fire hose, as jets of Circinus X-1 measured by Chandra. When the jets reach the gas of interstellar space, they seem to evolve to radio-emitting gas, which apparently carry huge amounts of kinetic energy, releasing through jet-matter interaction.

Matter falling onto the surface of an NS is thought to be along closed magnetic field lines contacting the accretion disk. However, the corresponding geometry of outflow is not well understood. Owing to the remarkable similarity between jets of BH and NS, it is possible that the outflow is also launched through open field line like the Blandford-Znajek effect (Blandford & Znajek 1977) in BH X-ray binaries. In such case, the spin of a NS affects the energy ejection at the line of sight (LOS), where the emission originated in shell collision is observed.

For an accreting NS system with opening angle of jet of $1/\Gamma \sim 10^\circ$, a misalignment angle between the jet axis

and the spin axis, around the same level, $\sim 10^\circ$, will not produce the pulsation like a pulsar, since the emission beam is never completely out of LOS. Obviously such a spin of NS results in the episodic ejection at LOS even if the jet is originally continuous.

Episodic ejection can also be reproduced by fluctuated accretion due to the interaction between the orbital motion of the flow and the NS rotation (Miller et al. 1998; Lamb & Miller 2001), which predicts a beat frequency, $\nu_b = \nu_K - \nu_s$ (where ν_K and ν_s are Keplerian frequency and spin frequency of NS respectively) responsible for high frequency QPO. In such case, the jet of such NS is not relevant with its pulsation, as displayed in the pulsar nebular of Crab.

Either of the two processes discussed above, can work as seed periodicity, so that shell collision can be generated in jet. In fact, the property of shell collision has been studied extensively in GRB prompt emission, which can be used in the case of QPO. Assuming a periodicity in the central engine, ejectors are launched out, in which a rapid shell (subscript r) catches up a slower one (s), and merge to a single one (m). The system behaves like an inelastic collision between two masses. By the conservation of energy and momentum, the Lorentz factor of the merged shell can be calculated (Kobayashi et al. 1997; Granot et al. 2012).

The evolution of the outflow can be studied by assuming that shells merge after collisions, which is approximately valid when all the internal energy generated by a collision of two shells is radiatively efficient (Zou et al. 2006; Li et al. 2008). As the flow radius increases, the typical number of initial shells that merge into one single shell increases, so that the variance of the Lorentz factors of the resulting shells decreases. In the case of numerous shells (much larger than that of Li & Waxman (Li et al. 2008)), the collision scenario is that fast shells with approximately same speed collide with a single shell which is relatively slow in speed and large in thickness and mass.

In the rest frame of the NS, the time scale of i -th collision between the rapid and merged shell (with dimensionless speeds β_r and β_m respectively) is given,

$$T_i = \frac{\Delta_{tot}}{c(\beta_r - \beta_m)} \quad (1)$$

where $\Delta_{tot} = \Delta_{gap} + \Delta_{sh}$, and Δ_{gap}/c and Δ_{sh}/c correspond to the period during which the central engine is off and on respectively.

Such an off and on can be realized by the flip jet axis. Suppose a shell is ejected between t_0 and $t_1 = t_0 + \Delta_{sh}/c$, at direction A ; and between t_1 and $t_2 = t_1 + \Delta_{tot}/c$, another shell is launched at direction B which deviates from A for a few degrees ... Consequently, for one circle of flip, there is one shell (ejector) launching out at time scale, $T_1 = (\Delta_{gap} + \Delta_{sh})/c$ (intrinsic time scale) at one direction.

In the co-moving frame of the rapid shell, the collision period of Eq.1 becomes,

$$T_2 = D_- T_i = \frac{D_- (\Delta_{tot})}{c(\beta_r - \beta_m)} = \alpha T_1 \quad (2)$$

where $\alpha = D_-/(\beta_r - \beta_m)$, the value of which will be dis-

cussed later, $D_- = 1/\Gamma(1 + \beta) = \sqrt{\frac{1-\beta}{1+\beta}}$ is the Doppler factor relating the rest frame of NS and the rapid shell of Lorentz factor Γ .

Transforming the period, T_2 , defined in the co-moving frame of the shell to observer's frame, we have,

$$T_{obs,2} = T_2 \Gamma(1 - \beta\mu), \quad (3)$$

where $\mu = \cos \theta(t)$, in which θ denotes the secular change of the misalignment angle between the jet axis and LOS. Further more, $T_{obs,2}$ corresponds to an oscillation frequency of, $\omega_2 = 2\pi/T_{obs,2}$. As the jet precesses, the misalignment angle between the jet axis and LOS, θ , varies, so that the specific intensity in comoving frame, F_* , is Doppler boosted and measured in observer frame as,

$$F_{obs} = D^3(t) F_* \exp(i\omega_2 t), \quad (4)$$

where $D(t) = 1/\Gamma\{1 - \beta \cos[\theta(t) + \delta\theta(t)]\}$ is the Doppler factor, where $\delta\theta(t) = \delta\theta_0 \exp(i\omega_1 t)$, with $\omega_1 = 2\pi/T_1$, represents rapidly flip of the jet axis relative to LOS. Apparently, the shell collision induced L-C, as shown in Eq.4, couples not only with two oscillations, ω_1 and ω_2 , but also with the angle θ . Thus, the PDS response of Eq.4 at different phase of jet precession (different θ), gives different frequencies of QPOs.

Notice that if the shell collision is due to spin induced flip, $\omega_1 = 2\pi/T_1$, the oscillation varies with shell thickness, which increases with increasing core-site separation. And in the case of beat frequency induced periodicity in jet, a constant ω_1 is expected, in which case, $\delta\theta(t)$ corresponds to fluctuated change of flux density given by Eq.4.

3. CONFRONTING WITH OBSERVATION OF 4U 1820-30

The collision described by the above equations occurs in the cone represented by the big ellipses as shown in Fig. 1, in which the instantaneous cone denoted by the small (yellow) ellipses flip in.

Launched at time, t_0 , the bulk speed of ejector i is $c\beta_i$. The ejector-core separation of site i at time t_i is $R_{\theta_i} = R_0 + c\beta(t_i - t_0)$. Owing to the jet precession, the neighboring sites of ejector i deviate from it both in direction and core-site separation. Such a continuous and precessing jet results in a spiral jet, as shown in Fig. 1, in which the collision site of kHz QPO is part of the spiral, from 3a to 3c, as shown in Fig. 1.

The jet precession towards left is equivalent to the motion of LOS at opposite direction as shown in Fig. 1. The onset of the shortest collision site corresponds to the start of kHz QPOs, which increase till saturation. After that, the increase of site-core separation, R_{θ_i} , reduces the collision frequency, which is responsible for the QPO frequency of a few Hz.

As shown in Fig. 1, the onset of sequence, 1,2,3 and 4 is observed due to the clockwise precession of jet. This explains the over all state change of 4U1820-30, the circle of island, low banana, upper banana of 4U1820-30. And the 176 days is apparently the precession period of jet as shown in Fig. 1.

Such a precession period can be satisfied by the long term effect of a binary system. E.g., the precession speed predicted by the geodetic precession (Barker & O'Connell

1975), is given by

$$\Omega = \frac{1}{2} \left(\frac{GM_{\odot}}{c^3} \right)^{2/3} \left(\frac{2\pi}{P_b} \right)^{5/3} m_c (4m_p + 3m_c) / (m_c + m_p)^{4/3} / (1 - e^2) \quad (5)$$

With orbital eccentricity $e = 0.65$, the orbital period $P_b = 11$ minute (685s) (Stella et al. 1987), and companion mass, $m_c = 0.06$ (Rappaport et al. 1987) (assuming $m_p = 1.4$), The precession period $P_p = 2\pi/\Omega \approx 176$ days can be satisfied.

Same precession period can be given by the Newtonian-driving precession (Larwood 1998) as well,

$$P_p = \left\{ \frac{3m_c}{7m_p} \left(\frac{r_d}{d} \right)^{3/2} \left(\frac{m_p}{m_p + m_c} \right)^{1/2} \cos \theta \right\}^{-1} P_b \quad (6)$$

with disk radius $r_d = 700r_s$ and the misalignment angle between accretion disk and orbital plane $\theta = \frac{\pi}{4}$, where r_s is Schwarzschild radius and d is the orbital separation.

At different θ , e.g., $\theta = 0.16$ rad, 0.27 rad, 0.35 rad, we can have corresponding PDS of the time series F_{obs} determined by Eq.4. This actually predicts the evolution of QPO frequencies versus θ . And due to the change of θ varies the counts through the effect of Doppler boosting as shown by Eq.4, the correlation of counts versus θ is a natural result.

Therefore, the evolution of the twin QPO frequencies versus the change of flux predicted by this model can be given by Eq.4, which can be compared with observation (Zhang et al. 1998) as shown in Fig. 2. The fitting parameters are given in Table 1, in which jet opening angle is relatively large and opening angle precession cone is not much larger than that of the jet and the amplitude of flip of the jet. Therefore, its emission never goes down below observation threshold. Under such a configuration, QPO can exist for the majority part of the precession period for this source, which well account for the observation (Zhang et al. 1998).

The PDS of Eq.4 at different θ is shown in Fig. 2. This numerical result indicates that the lower QPO corresponds to the frequency of shell collision, $\omega_2/2\pi$; and the upper one corresponds to the coupling between the frequency of shell collision and the intrinsic frequency $\omega_2/2\pi + 1/T_1$.

The frequency discrepancy between the twin kHz QPOs is $\nu_u - \nu_L = 1/T_1 \simeq 275$ Hz, in which T_1 is a parameter related with the seed periodicity of the NS system. The frequency ratio between the twin QPOs is, $\nu_u/\nu_L = 1/(T_1\nu_L) + 1$, which can decrease from 1.6 to 1.3 with the increase of ν_L from 450 Hz to 800 Hz. This is consistent with observations of 4U 1820-30 (Barret & Boutelier 2008).

This scenario explains not only the increase of QPO frequencies (Zhang et al. 1998), but also its correlation with change of flux. As shown in Fig. 1, when the slashed ellipse and ellipses near the sign 3a is precessing close to LOS, the first collision site of kHz QPO (with shortest core-site separation) is onset. This actually corresponds to a decrease of θ , and accordingly an increase of ω_2 as given by Eq.3. Until its minimum θ_{min} is reached between 3b and 3c of Fig. 1.

Later on, θ , the misalignment angle of the first collision site and LOS, continues increase, so that LOS is aligning with collision site of larger core-site separation as denoted by 3c in Fig. 1.

In such case, the collision parameters of Eq.1-Eq.4 are unchanged, and hence the kHz QPO frequency is unchanged. During this process, the soft emission from the disc contributes to the flux, which explains the saturation of QPO frequency with increase of flux (Zhang et al. 1998).

A gap around the point (600,900) Hz in correlation line that links the upper QPO frequency to lower QPO frequency is reported (Barret & Boutelier 2008), in which twin kHz QPOs are absent.

This process corresponds to the LOS denoted by 3b in Fig. 1, in which the first collision site and its adjacent sites (of larger core-site separation) are aligned with LOS simultaneously (recall large opening angle of the jet). The superposition of the time series of such multi-site may result in noise feature in PDS, which explains the QPO gap (Barret & Boutelier 2008; Belloni et al. 2005).

In this new scenario, random process is involved both in splitting the continuous jet into discrete shells (ejectors), and in shell collision process. Moreover, the clump in the accretion of NS systems also contaminates the signal randomly.

On the other hand, with parameters of Table 1 and a speed discrepancy of $\beta_r - \beta_m \approx 17\% \sim 6\%$, the parameter α is confined approximately between 1~3. If α deviates from 1~3 significantly, the QPO frequency would be much lower, or much higher than kHz respectively, which can be both ruled out for the case of 4U 1820-30.

All these factors contribute to the multiple peaks of kHz QPO, which is consistent with the overall distribution of peaks of QPO (Belloni et al. 2005). In fact, the new model predicts that multiple peaks of kHz QPO exist during the whole evolution of kHz QPOs, which can be tested by further data analysis.

The frequency discrepancy in some LMXB systems (e.g., Sco X-1) becomes flat at higher frequency range (Lin et al. 2011). This can be naturally explained by the increase of the shell thickness, Δ_{sh} , which increases T_1 , and reduces the frequency discrepancy between the twin QPOs. At the same time, QPO frequencies increase owing to the decrease of θ . Consequently, the change of frequency discrepancy of Sco X-1 (Lin et al. 2011) can be interpreted as the evolution T_1 , as shown in Fig. 3(c).

The QPO frequency of 7 Hz observed in 4U 1820-30 (Belloni et al. 2004), can also be interpreted by the increase of core-site separation and hence increase of the shell thickness, Δ_{sh} , and T_1 , and thus low QPO frequency. Obviously, such low oscillation frequency can occur at state after state 3c and before state 1 as shown in Fig. 1.

As a measure of the signal strength, the root-mean squared (RMS) amplitude is proportional to the square root of the peak power contribution to the PDS. The evolution of RMS at different θ can be obtained through Eq.4 either. As shown in Fig. 3(a), the trend of the evolution of RMS of the lower QPO frequency is consistent with the observation (Török 2009). Although the absolute amplitude of RMS in the numerical calculation is much larger than that of observation, owing to the signal to noise ratio of simulated signal is much stronger than that of true data.

TABLE 1
THE FITTING PARAMETERS FOR THE QPO MODEL

$\lambda(\text{rad})$	$i(\text{rad})$	$T_1(\text{ms})$	Γ	$\delta\theta_0(\text{rad})$	α
0.29	0.14	3.6	3.0	0.3	1.7

NOTE: λ is the opening angle of jet precession, i is the misalignment angle between jet rotation axis and LOS, Γ is the Lorentz factor of jet and $\delta\theta_0$ is flip amplitude of jet.

4. DISCUSSION AND PREDICTION

In such a simple scenario, with six parameters as shown in Table 1, the evolution of the twin kHz QPO versus counts is simulated as shown in Fig. 2, which explains the correlation of the twin kHz QPOs with the luminosity, and hence the spectral state of 4U 1820-30. Simultaneously, it also explains the RMS trend of the lower QPO, as shown Fig. 3(a). The fitting of Fig. 3(a) and Fig. 2 together suggests that the observational feature of twin QPOs can be reproduced simply by an emission site suffering Doppler effects, which in turn suggests that kHz QPO may originated in shell collision in jet of X-ray binaries.

In this model, the state of a source with jet precession can be represented by the misalignment angle between the jet axis and LOS, e.g., $\theta = 0.16\text{rad}$, which corresponds to the parameter, S_a , measuring the position of

an atoll source within its CCD (Hasinger & van der Klis 1989). As a result, the model can be tested by the time elapsed between states (denoted by different θ , and hence different S_a), as predicted by 2 and Fig. 3(a).

The simulation of PDS of Eq.4 also exhibits a QPO with frequency, $\nu = \nu_L - 275\text{Hz}$, as denoted by dashed peak in Fig. 3(b). With a lower RMS amplitude, the predicated frequency can vary at the range, 325~525Hz, as ν_L changes at the range of 600~800Hz. The measurement of such predicted QPO frequency will be direct test of the model.

We thank B. Zhang, Z. Li, Y.C. Zou and W.H. Lei for helpful discussions. This research is supported by the National Natural Science Foundation of China, under grand NSFC11178011.

REFERENCES

- Abramowicz, M. A., Karas, V., Kluzniak, W., Lee, W. H., Rebusco, P.2003, PASJ, 55, 467
 Bachetti, M., Romanova, M. M., Kulkarni, A., Burderi, L., di Salvo, T.2010, MNRAS, 403, 1193
 Barker, B.M. & O'Connell, R.F. 1975, Phys.Rev.D., 12, 329
 Barret, D., & Boutelier, M.2008, New Astron. Rev., 51, 835
 Belloni, T., Mendez, M., & Homan, J.2005, A&A, 437, 209
 Belloni, T., Parolin, L., & Casella, P., 2004, A&A, 423, 969
 Blandford R.D., & Znajek R.L. 1977. MNRAS179,433
 Hasinger, G. & van der Klis, M. 1989 A&A,225,79
 Gong, B. P., Kong, S. W., Xue, F., Li, Y. P., & Huang, Y. F.2011, MNRAS, 418, 2451
 Granot, J., 2012, MNRAS, 421, 2467
 Lamb, Frederick K. & Miller, M. Coleman 2001, ApJ, 554, 1210
 Larwood, J. 1998, MNRAS, 299, L32
 Li, Z. & Waxman, E.2008, ApJ,674, L65
 Lin, Y.F., Boutelier, M., Barret, D., Zhang, S.N.2011, ApJ, 726, 1
 Mendez, M., van der Klis, M., van Paradijs, J.1998, ApJ, 506, L117
 Miller, M. Coleman, Lamb, Frederick K., & Psaltis, Dimitrios 1998, ApJ, 508, 791
 Kobayashi, S., Piran, T., & Sari, R., 1997, ApJ, 490, 92
 Priedhorsky, W., Terrell, J.1984, ApJ, 284, L17
 Rappaport, S., Ma, C. P., Joss, P. C., Nelson, L. A.1987 ApJ, 322, 842
 Simon, V.2003, A&A, 405,199
 Stella, L., Priedhorsky, W., White, N. E. 1987, ApJ, 312, L17
 Török, G. 2009, A&A,497, 661
 van der Klis, M., Wijnands, Rudy A. D., Horne, K., Chen, W.1997, ApJ, 481, L97
 Zhang, W., Smale, A. P., Strohmayer, T. E., Swank, J. H.1998, ApJ, 500, L171
 Zou, Y. C., Dai, Z. G., Xu, D.2006, ApJ, 646, 1098

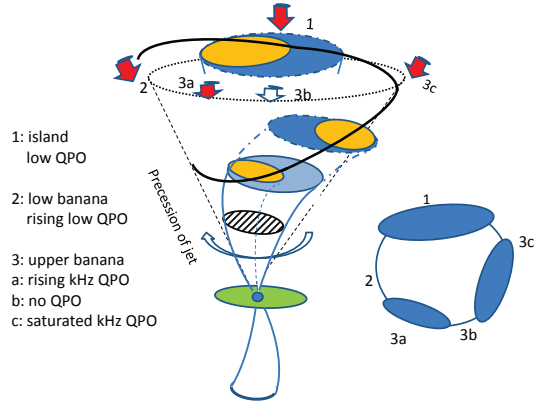


FIG. 1.— Schematic plot of the precession geometry of LMXB 4U1820-30. The opening angle of the jet is denoted by the small ellipse, and its range of flip is represented by the large ellipse. The jet precesses at a 176 days period, towards left, which is equivalent to the motion of LOS at opposite direction. The states of CCD correspond to different misalignment angle of the jet to LOS.

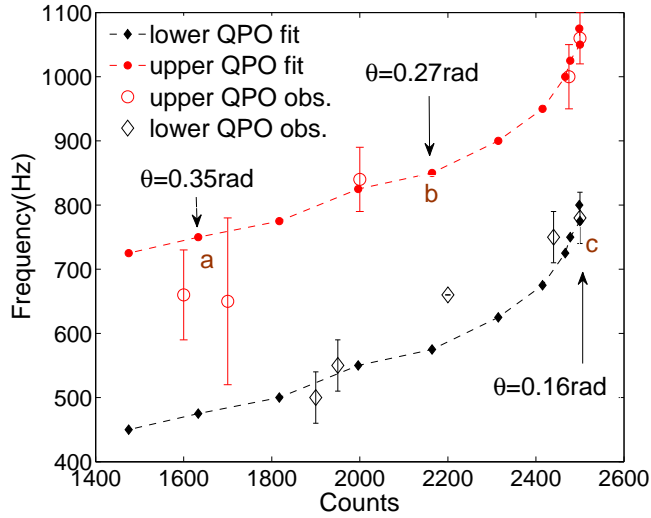


FIG. 2.— Observed and fitted QPO centroid frequencies versus count rate. Observational data is from Zhang et al. (1998). Different misalignment angle between LOS and jet axis, θ , determines twin kHz QPO frequency and counts through Eq. 4. The time elapsed in the observer's frame at point *b* and point *c* from *a* are 16.3days and 37.0days, respectively.

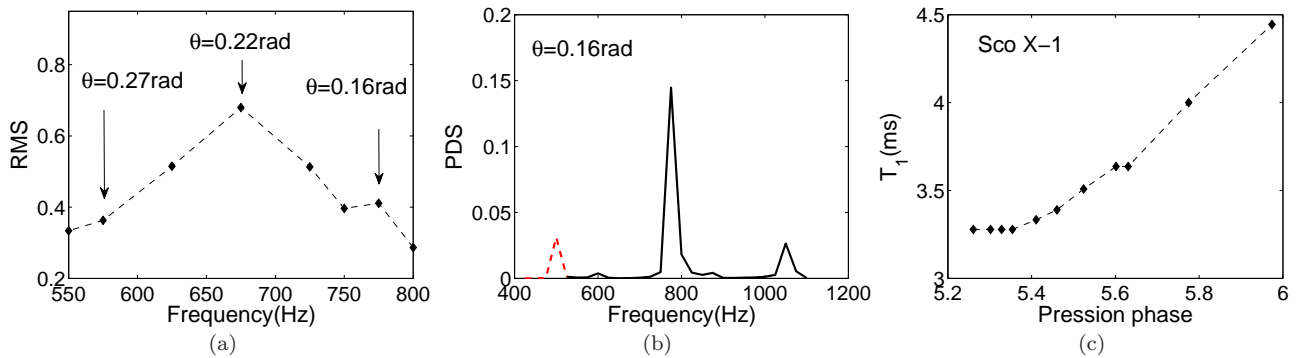


FIG. 3.— (a). Fitted RMS versus lower QPO frequency consisting with the observed trend of 4U 1820-30 (Török 2009). The time elapsed between $\theta = 0.27$ and $\theta = 0.22$ is 9.0days. (b). Power Density Spectrum of 4U 1820-30 for a specific precession state with $\theta = 0.16$ rad. The predicated QPO frequency is indicated by the red dashed peak. (c). The evolution of T_1 with precession phase responsible for the frequency relationship of Sco X-1 (Lin et al. 2011).